DOUBLE MICRORING RESONATORS POLYMER WAVEGUIDE FOR OPTICAL BIOSENSING

Mohd Hazimin Mohd Salleh[1*], Mohd Haziq M.Salleh[2], Muhammad Salihi Abd Hadi[3]

[1]*Department of Physics, Kulliyyah of Science, International Islamic University Malaysia (IIUM), 25200 Kuantan, Pahang, Malaysia*

[2]*Department of Computer Science, Kulliyyah of Information and Communication Technology, International Islamic University Malaysia (IIUM), Gombak, 50728 Kuala Lumpur, Malaysia*

[3]*Department of Computational and Theoretical Science, Kulliyyah of Science, International Islamic University Malaysia (IIUM), 25200 Kuantan, Pahang, Malaysia*

[*]*Corresponding author: mhazimin@iium.edu.my*

Abstract

The potential of double microring resonator polymer waveguide as an optical biosensor was demonstrated. Visible wavelength region at 632 nm is used as a centre wavelength because it is commonly used in biological and chemical sensing for both label and label-free sensing. The double microring resonator waveguide structure is simulated using COMSOL Multiphysics optical design and analysis software. The results show that there is a transmission drop with a 3 dB bandwidth of 631.4 nm when the surrounding refractive index is 1.33. The specific wavelength (output transmission) is shifted to 674.6 nm when the surrounding medium into 1.43, in order to imitate the bioanalytes solution. According to simulation result, the wavelength shift was approximately 43.2 nm for 0.1 increasing of surrounding refractive index. The double microring resonator polymer waveguide was fabricated by using electron beam lithography. Then, the fabricated devices were integrated into microfluidic systems in order to validate the wavelength shift. From the experiments, the wavelength shift occurred approximately 32.3 nm over 0.1 increment of refractive index. Thus both simulation and experimental results strongly indicate that double microring resonator polymer waveguide structure at visible wavelength region have a potential for label or label-free optical biosensing applications.

Keywords: Optical biosensor, COMSOL Multiphysics, double microring, label-free, polymer waveguide.

Introduction

Currently, the application of rapid sensing and detection of biological analytes are growing due to the significant environment monitoring, biological screening and biochemical sensors. These factors inspired research and development upon simple, cheap and sensitive functional biomolecular device at very low concentration sample. Meanwhile, the interest in label-free optical detection has increasing since the planar waveguide has a direct light interaction with surrounding medium, easy integration with microfluidic system and the capability to provide specific interaction (Rodrigues et al., 2015; Donzella et al., 2015 and Chen et al., 2015). Basically, a planar waveguide employs an evanescent field on a waveguide surface to interact with analytes of surrounding media. In order to identify a low concentration of active analytes, it

is essential to have an extensive detection surface area but at the same time reducing the dimension of the device. Among the planar optical biosensors, microring resonator has attracted much interest due to its structure, which offers both the quality of smaller size and further enhancing the sensing surface area (Dantham et al., 2012 and Baaske et al., 2012). One of the important characteristics of microring resonator is the strong evanescent modes can be achieved out of waveguide surface without tapering or etching process, which increase the tendency of strong evanescence field to interact with bio-analytes.

Generally, silicon nitrides, silicon oxide, silicon-on-insulator (SOI), Hydex Glass are the mainstream materials for core waveguide of microring resonator structure. However, silicon-based material is not transparent to the visible light region (Ramachandran et al., 2008; Wang et al., 2015; Vollmer et al., 2002 and Hanumegowda et al., 2005). For example, silicon based microring resonator waveguide only exists at the communication wavelength region (1500nm). In addition, silicon based material also requires several steps of fabrication process (reactive ion etching (RIE), mask layer deposition etc), which make it complicated to prepare and time consuming compared to polymer-based material (Xia et al., 2008; Yalcin et al., 2006; Xu et al., 2010 and Ahmed et al., 2016). As mentioned earlier, in optical biological sensing, evanescence field on the top surface of waveguide plays very crucial part for light and analytes interaction. For that reason, microring resonator has drawn attention for optical biosensors. Various designs and materials have been used to fabricate the structures.

Furthermore, the polymeric based materials offer several advantages over the silica based materials, in terms of their straightforward fabrication process, good surface modification for analytes immobilization and a wide selection of refractive indices (Sun et al., 2008; Salleh et al., 2013 and Salleh et al., 2016). Several polymers have been used in microring resonator fabrication such as polymethyl-methacrylate (PMMA), polystyrene (PS) and SU8. However, in this paper, SU8 polymer (MicroChem Corporation) was utilized as a core structure for microring resonator and straight waveguide. Because SU8 is a negative tone photoresist, an exposed area will be remained on the substrate after the development process.

In this paper, a label-free optical detection in biosensing was studied by using polymer double microring resonator waveguide as a sensing structure. The change of refractive index of liquid sample was used to mimic the protein interaction around sensing area. The optical responses of output waveguide were characterized after refractive index of sensing area was changed purposely. The visible wavelength region was utilized as a light source to determine the capability of the device.

Materials and Methods

Fabrication

The SU8 polymer double microring resonator waveguide was fabricated on 3.5 μm oxide of wafer by using electron beam lithography (EBL) in James Watt Nanofabrication Centre (JWNC, University of Glasgow) [15-16]. First, the substrates were cleaned ultrasonically by using acetone and Isopropyl alcohol (IPA) for 5 minutes each. Then, the substrates were rinsed by reverse osmosis (RO) water. The substrates were put in the oven at 180^{o}C for 5 minutes to dry. Next, the substrates were treated in the oxygen plasma at 100 W, for 5 minutes. The SU8 resist was spun at 3000 rpm for 30 sec, and then soft baked for 2 minutes at 95^{o}C to evaporate the coating solvent and firm down the resist on the top of the SiO_2 after coating. The substrates were

cooled down under room temperature before can be patterned. After electron beam patterning, substrates were pre-exposure baked (PEB) for 1 minute at 65^{o}C and 1 minute at 95^{o}C and usually SU8 pattern should be visible on the resist surface after PEB process. The SU8 pattern were developed with EC solvent (Ethyl 2-hydroxypropanoate) for 2 minutes, followed by 1 minute of Isopropyl Alcohol (IPA) and dried with nitrogen gun. As a final step, hard-baked was performed at 180^{o}C on the hotplate for 5 minutes. The fabricated patterns were shown in Figure 1. The fabricated substrates were cleaved and aligned for further experiments

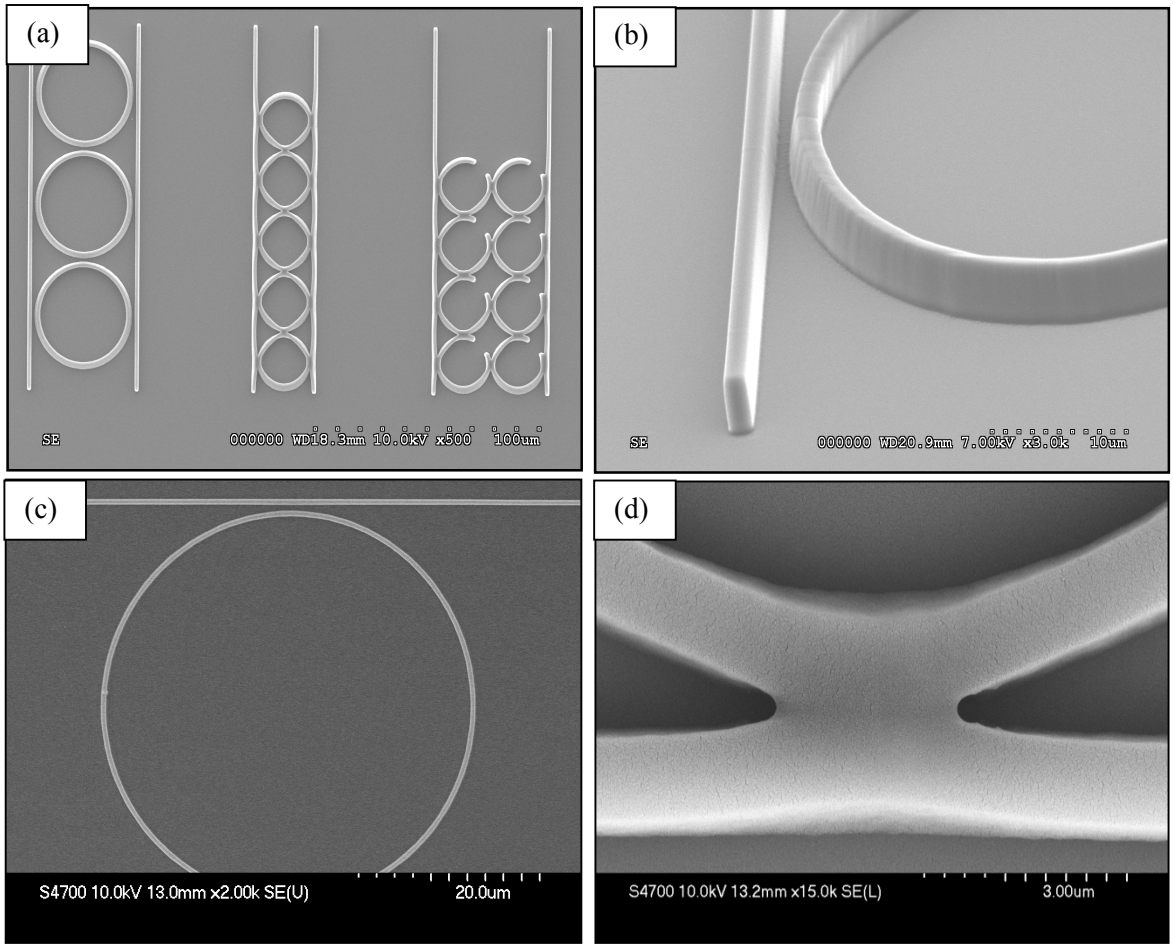

Figure 1. Scanning electron microscopy (SEM) images show the fabricated structure of SU8 polymer waveguide; (a) Multi-ring resonator at different radius, x0.3k magnification, (b) High aspect ratio structure and sidewall of waveguide, x3.0k magnification, (c) Gap between bus and ring resonator arrangements, (x3.0k magnification), and (d) Gapless ring with 40 μm radius, x10.0k magnification

Experimental Setup

The experimental setup consists of devices as depicted in Figure 2. It is mainly of two parts; controlling the optical component and manipulating the liquid samples. As described earlier, the fabricated sensors were characterized by using visible wavelength spectrum using end-facet technique. First part, an optic lamp (100W, 12V, Osram) was used as the main visible light source. HeNe laser (Melles Griot, 5mW) was collimated into the input waveguide and then exploited as a guiding light source for alignment and calibration process. After that, coupling fiber from HeNe laser was shifted to visible light, and visible source will be used as a major source for detection. Translation stage was employed in order to align the light guiding inside the waveguide for both input and output waveguides. Spectral output from the opposite side of input waveguide was collimated into 20X objective lens that was projected onto the fiber optics collector. Then, the output signal was propagated onto the spectrum analyzer (500M, Jobin Yvon Horiba) and captured by charged-coupled device (CCD) (Andor, DU420-BR-DD) camera. Next, the optical responses were scanned and recorded for further analysis. Meanwhile, microfluidic channel system was constructed in order to inject the liquid sample into the sensor surface. Then, the flow of liquid was controlled by programmable syringe pump (World Precision Instrument, AL-1000). Finally, liquid was injected through the microfluidic channels covering the sensing area and then streamed into the waste bottle (Eppendorf tube).

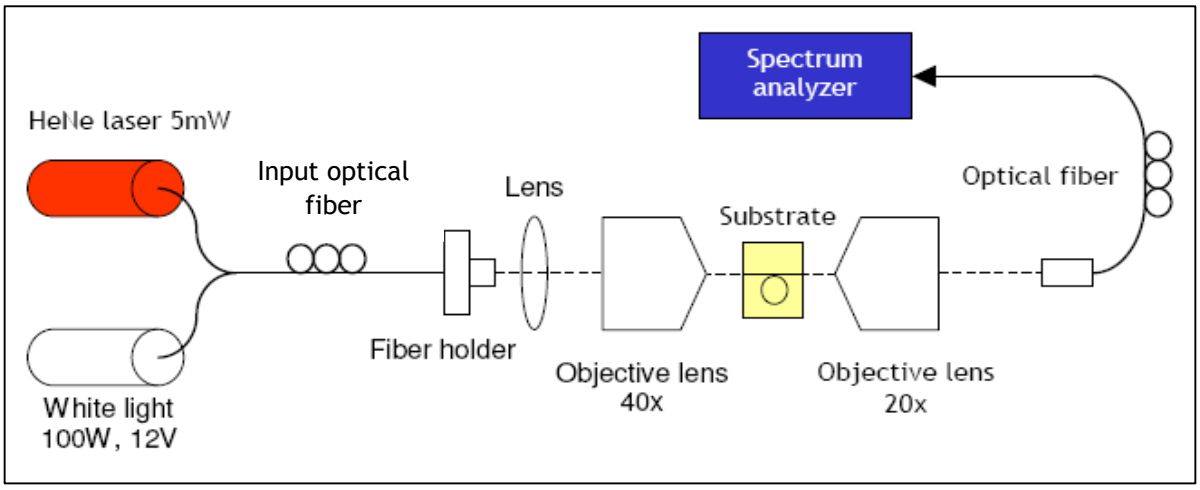

Figure 2. Schematic diagram of the measurement setup used for device characterization and experiments.

In order to conduct the experiment, HeNe laser is used both for calibration and in experimental work. Laser is used for input and output coupling alignment; the substrate (consist of fabricated double microring resonator) is manipulated using a 3-axis stage to achieve the highest reading. When the maximum intensity is obtained from the spectrum analyser, the input fiber is switched to the white light source.

Results and Discussion

Simulation

The commercially available COMSOL Multiphysics simulation software was utilized to simulate the spectrum response. The structure of double microring resonator waveguide was modelled. The Gaussian pulse was centered at vacuum wavelength of 632 nm was launched into the designated input port. The spectral responses (transmission) of the double microring resonators were obtained from output port. The device refractive index was set at 1.57 to mimic the polymer material and surrounding area was set up at 1.33 to represent water. The surrounding refractive index of sensing area (been immobilized with protein in earlier) will be increased when specific biological binding occurred. This means that more bioanalytes deposited and covered the sensing surface area. In simulation, the refractive index of surrounding area was numerically increased to imitate the biomolecular binding interaction on the sensing area. According to the double microring resonator model, the change of effective index of the cladding / sensing area (in this paper, it was polymer surface), will directly shift the resonance wavelength. From this hypothesis, the spectral response from the input were simulated and recorded, as depicted as output and drop port. Figure 3 shows the normalized intensity (a.u) of transmission spectral of polymer double microring structure within the visible wavelength region. The simulated device structure parameters consist of waveguide width at 2 um, ring radius of r_1 = 45 µm and of r_2 = 46 µm. By increasing the refractive index of surrounding medium from 1.3330 to 1.3478, the transmission spectrum was shifted to the right of the spectrum region as depictured in Figure 3. Then the refractive indexes were gradually increased until 1.4200. From the simulation, the spectral shift stretches approximately to 53.7 nm due to the increase of approximately 0.1 refractive index of surrounding sensing area.

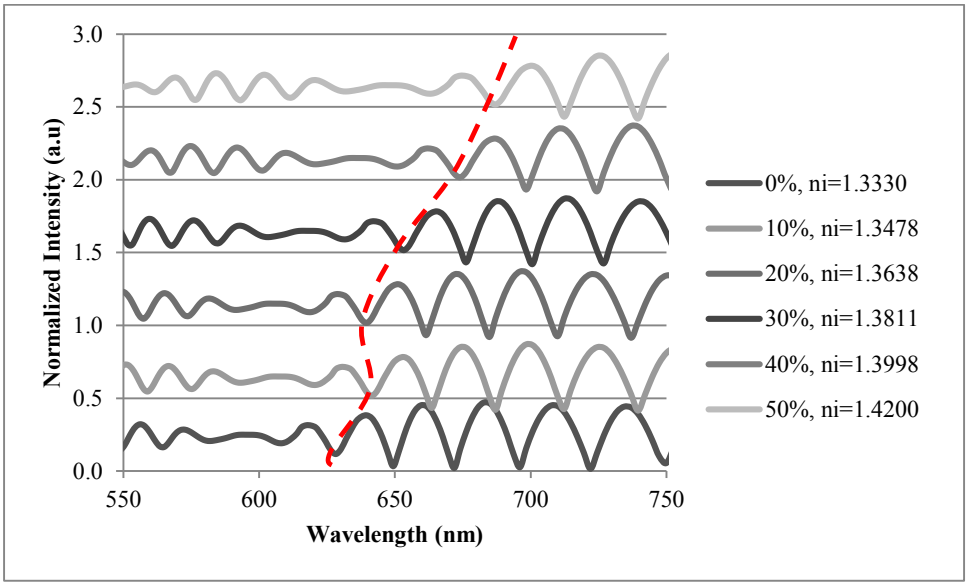

Figure 3. Simulated spectral response (transmission spectra) of double microring resonators device.

The simulated spectral response as transmission spectra of double microring resonators device within the visible wavelength region was presented. Spectral shift pathway (red dashed line) due

to the refractive index changes of surrounding sensing medium. The spectral shift (from left to right) occurred at different refractive index respectively

Experimental

In order to demonstrate the capability of the device as a biosensing, experiment was carried out to characterize the fabricated double microring resonator with the dimension of 2 x 2 um (width x height). Figure 4 shows the normalized intensity (a.u) of spectral shift response of double microring resonators waveguide within the visible wavelength region. In order to clarify the measurement of the resonance shift, the recorded spectra in Figure 4, where the y-axis was expanded and resonance peak was traced up to make it easier to see the shift in resonance peak. Since the base solution for this experiment was the DI water, the initial resonance response at t = 0 s was recorded when the sensor area was filled with the DI water. A reference spectral drop was measured at λ = 600.560 nm. The concentrations of the mixed sucrose solution corresponding to these measurements were derived from Table 1.

Table 1. The result of sucrose concentration solution, refractive index measurement and spectral shift (nm) from experiment and simulation.

Sucrose solution (%)	Refractive index*	Spectral shift, nm	
		Simulation	Experiment
0	1.3333	0	0
10	1.3478	15.1010	0
20	1.3638	13.1744	21.760
30	1.3811	26.9085	21.760
40	1.3998	37.0853	38.080
50	1.4200	53.7239	38.080

* Abbe refractive index

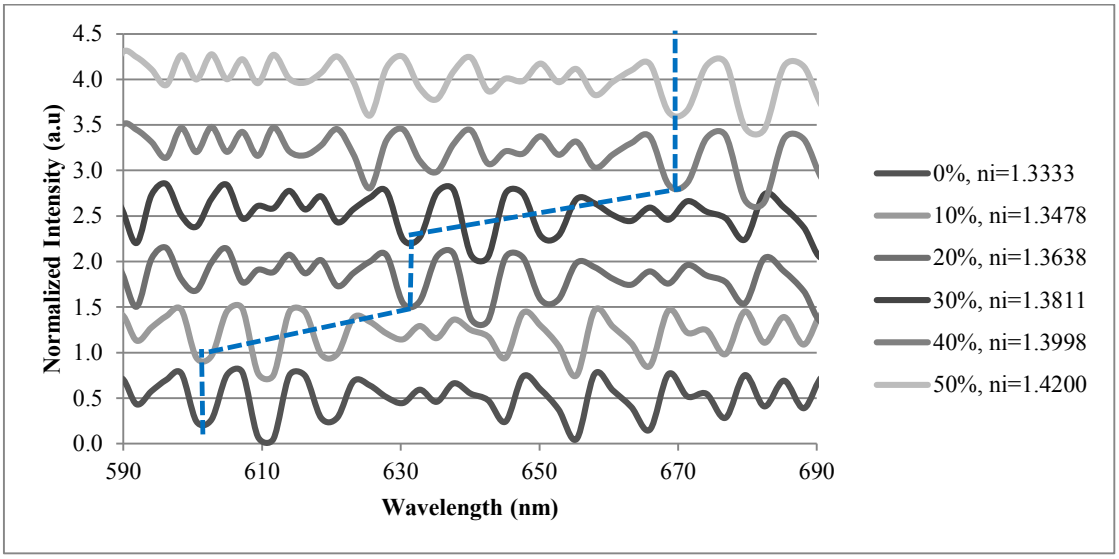

Figure 4. Normalized intensity of resonance wavelength pattern at different mixing stage period (%) of experiment.

According to the Figure 4, the wavelength region was projected between λ = 630 – 700 nm. The plotted lines were vertically displaced for the ease of comparison. The (blue dashed line) shows the tracked of spectral drop position upon the time duration and mixing stage percentage of sucrose at increasing concentration profile.

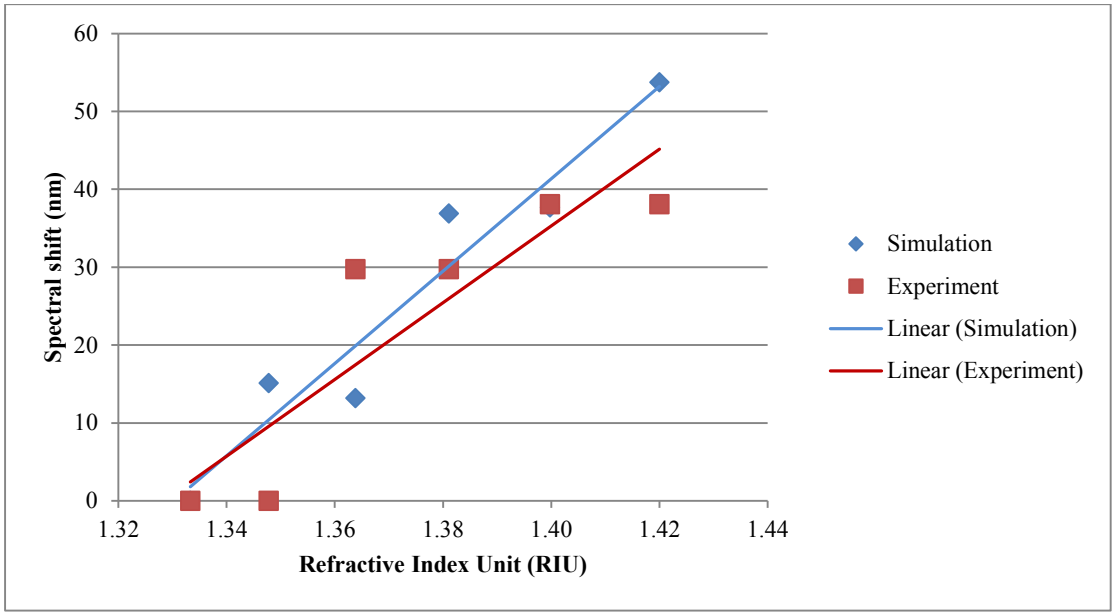

Figure 5. Comparison of spectral shift between simulation and experimental characterization of double microring resonator waveguide at specific refractive index of surrounding sensing area.

From the obtained results, it is appeared that the spectral shifts for the pre-made 10, 20 and 30% solutions make an over estimate of the sucrose concentration. For comparison between simulation and experimental works, graph was plotted as in Figure 5. According to Figure 5, spectral shift responses for both COMSOL simulation and experiment show an increasing pattern of spectral shifts upon sucrose refractive index, as shown in Table 1.

The spectral shift groups obtained from the experiment were compared to COMSOL Multiphysics simulation results at certain refractive index unit. According to the experiment, the spectral shift was occurred dramatically with increment of the sucrose concentration at 10% to 20% and 30% to 40%. Meanwhile, the tracking spectral positions remain unchanged at sucrose concentration from 20% to 30% and 40% to 50%. The discrepancies suspected likely due to the accumulation of pre-mix solution on top and sidewall of the sensing area, causing the interaction of evanescent tail attenuated due to increasing of sucrose concentration injection into the microfluidic system. Another potential factor that affects experimental value were the optical resolution of the spectrometer and sidewall roughness of the double microring resonators respectively, that enriched the noise to signal ratio.

In order to overcome these hurdles, higher resolution optical spectrometer need to be utilized and smoothing the sidewall roughness of the resonator structure by improving the fabrication steps. These practice, hopefully will lead to better precision in the determination of spectral shifts especially in experiment.

As initial results, a linear relationship shows between the spectral shifts within the visible wavelength region and the sucrose refractive index value. The capability of double microring resonator structure to sense the RI changes of sensing area with straight forward fabrication process was successfully presented. Visible wavelength region also has huge potential to facilitate the optical measurement for both label and label-free biosensing applications.

Conclusions

In this study, the SU8 polymer double microring resonator waveguide as optical biosensing was demonstrated. The straightforward procedure of SU8 polymer fabrication process has revealed an important role in rapid fabrication steps without performing a number of fabrication stages and layers. The device was validated by simulating the double microring resonator waveguide, performing the experiment upon the polymer fabricated device and monitoring the output spectral response in real time. Both simulation and experiment were based on variation of refractive index of sucrose concentration solution. It was demonstrated that the fabricated waveguide could be used to measure the refractive index of a sucrose solution (bulk detection). When the refractive index of the surrounding sensing area was changed (concentration increment of sucrose solution), the spectral shift occurred by approximately 53 nm (simulation) and 38 nm (experiment) with the increment of 0.1 refractive index unit. Future work will include the system to monitor changes in the refractive index of surrounding media and specific proteins interaction.

Acknowledgment

The authors would like to thank Bioelectronics Group and James Watt Nanofabrication Centre (JWNC) staff and technicians, Glasgow University. The acknowledgement also goes to International Islamic University Malaysia (IIUM) and Ministry of Higher Education Malaysia (MOHE) for fully funded RIGS Grant (RIGS 16-103-0267*),*

Conflict of interests

The authors would like to clarify that we have NO affiliation with or involvement in any organization or entity with any financial interest for supporting this research except were already fully acknowledged.

References

Ahmed, R., Rifat, A. A., Yetisen, A. K., Salem, M. S., Yun, S. H., & Butt, H. (2016). Optical microring resonator based corrosion sensing. *Rsc Advances*, *6*(61), 56127-56133.

Baaske, M., & Vollmer, F. (2012). Optical resonator biosensors: molecular diagnostic and nanoparticle detection on an integrated platform. *ChemPhysChem*, *13*(2), 427-436.

Chen, Y., Yu, F., Yang, C., Song, J., Tang, L., Li, M., & He, J. J. (2015). Label-free biosensing using cascaded double-microring resonators integrated with microfluidic channels. *Optics Communications*, *344*, 129-133.

Dantham, V. R., Holler, S., Kolchenko, V., Wan, Z., & Arnold, S. (2012). Taking whispering gallery-mode single virus detection and sizing to the limit. *Applied Physics Letters*, *101*(4), 043704.

Donzella, V., Sherwali, A., Flueckiger, J., Grist, S. M., Fard, S. T., & Chrostowski, L. (2015). Design and fabrication of SOI micro-ring resonators based on sub-wavelength grating waveguides. *Optics express*, *23*(4), 4791-4803.

Hanumegowda, N. M., White, I. M., Oveys, H., & Fan, X. (2005). Label-free protease sensors based on optical microsphere resonators. *Sensor Letters*, *3*(4), 315-319.

Ramachandran, A., Wang, S., Clarke, J., Ja, S. J., Goad, D., Wald, L., ... & Gill, D. (2008). A universal biosensing platform based on optical micro-ring resonators. *Biosensors and Bioelectronics*, *23*(7), 939-944.

Rodriguez, G. A., Hu, S., & Weiss, S. M. (2015). Porous silicon ring resonator for compact, high sensitivity biosensing applications. *Optics express*, *23*(6), 7111-7119.

Salleh, M. H., Glidle, A., Sorel, M., Reboud, J., & Cooper, J. M. (2013). Polymer dual ring resonators for label-free optical biosensing using microfluidics. *Chemical Communications*, *49*(30), 3095-3097.

Salleh, M., Hazimin, M., Mohd Salleh, M. H., Hadi, A., & Salihi, M. (2016). Optical biosensors prospective based on Bragg grating polymer waveguide. *Jurnal Teknologi*, *78*(3), 141-147.

Sun, Y., Shopova, S. I., Frye-Mason, G., & Fan, X. (2008). Rapid chemical-vapor sensing using optofluidic ring resonators. *Optics letters*, *33*(8), 788-790.

Vollmer, F., Braun, D., Libchaber, A., Khoshsima, M., Teraoka, I., & Arnold, S. (2002). Protein detection by optical shift of a resonant microcavity. *Applied physics letters*, *80*(21), 4057-4059.

Wang, J., Yao, Z., & Poon, A. W. (2015). Silicon-nitride-based integrated optofluidic biochemical sensors using a coupled-resonator optical waveguide. *Frontiers in Materials*, *2*, 34.

Xia, Z., Chen, Y., & Zhou, Z. (2008). Dual waveguide coupled microring resonator sensor based on intensity detection. *IEEE Journal of Quantum Electronics*, *44*(1), 100-107.

Xu, D. X., Vachon, M., Densmore, A., Ma, R., Delâge, A., Janz, S., ... & Liu, Q. Y. (2010). Label-free biosensor array based on silicon-on-insulator ring resonators addressed using a WDM approach. *Optics letters*, *35*(16), 2771-2773.

Yalcin, A., Popat, K. C., Aldridge, J. C., Desai, T. A., Hryniewicz, J., Chbouki, N., ... & Gill, D. (2006). Optical sensing of biomolecules using microring resonators. *IEEE Journal of Selected Topics in Quantum Electronics*, *12*(1), 148-155.